RESEARCH ARTICLE



Zinc hyperaccumulation in *Cardamine waldsteinii* from the Western Balkans: a field and synchrotron investigation

Ksenija Jakovljević · Mirko Salinitro · Sandro Bogdanović · Siniša Škondrić · Tomica Mišljenović · Antony van der Ent

Received: 12 July 2025 / Accepted: 13 October 2025 © The Author(s) 2025

Abstract

Background and aims Zinc hyperaccumulation is a very rare phenomenon on nature known from only 20 taxa around the World, especially in the genus *Noccaea* (Brassicaceae). *Cardamine waldsteinii* is a recently discovered (hyper)accumulator of zinc from central Europe and the Balkans. This study aimed to determine the ability of zinc hyperaccumulation in wild populations of *C. waldsteinii* and to elucidate its internal distribution in plant organs and tissues.

Methods Plant and associated soils samples from the native habitat of *C. waldsteinii* in the Western Balkans were collected and analysed to determine Zn accumulation. This was coupled with synchrotron micro-X-ray fluorescence elemental imaging, to elucidate the distribution of zinc in the plant organs.

Responsible Editor: Paula Pongrac

K. Jakovljević

Department of Ecology, Institute for Biological Research, Siniša Stanković – National Institute of the Republic of Serbia, University of Belgrade, Belgrade, Serbia

M. Salinitro · A. van der Ent (☒) Laboratory of Genetics, Wageningen University and Research, Wageningen, The Netherlands e-mail: antony.vanderent@wur.nl

Published online: 11 November 2025

S. Bogdanović

Department of Agricultural Botany, University of Zagreb Faculty of Agriculture, Zagreb, Croatia

Results The results confirm that *C. waldsteinii* is a genuine zinc hyperaccumulator meeting all established criteria for hyperaccumulation. The endodermis and vascular bundles were the main sites of zinc localisation in the roots and in the stem, whereas in the leaves the marginal areas were the most zinc enriched.

Conclusions We confirm the hyperaccumulation properties of *C. waldsteinii* in wild populations, whilst synchrotron micro-X-ray fluorescence elemental imaging reveal the zinc localisation patterns in organs and tissues. This study highlights the need for a comprehensive study of the genus *Cardamine* with the aim of discovering new metal/metal-loid hyperaccumulator species.

Keywords Hyperaccumulator · Elemental localisation · Synchrotron-based X-ray fluorescence imaging

S. Škondrić

Faculty of Natural Sciences and Mathematics, University of Banja Luka, Banja Luka, Bosnia and Herzegovina

T. Mišljenović

Institute of Botany and Botanical Garden, Faculty of Biology, University of Belgrade, Belgrade, Serbia

A. van der Ent Université de Lorraine, INRAE, 54000 Nancy, LSE, France



Introduction

Cardamine waldsteinii Dyer (Brassicaceae) is a newly discovered Zn accumulator from Central Europe and the Balkans with up to 3050 $\mu g \ g^{-1} \ Zn$ in herbarium material revealed by handheld X-ray fluorescence (XRF) analysis, compared to 2210 μ g g⁻¹ in the leaves of this species collected in the field (Jakovljević et al. 2023). To date, foliar concentrations of Zn in excess the 3000 μ g g⁻¹, which is the nominal threshold for hyperaccumulation of this element (van der Ent et al. 2013), have been found in only approximately 20 taxa globally (Reeves et al. 2018), compared to ~700 plant taxa known to hyperaccumulate metals/metalloids globally (Reeves et al. 2018). Zinc is an essential element for plants, the second most abundant transition metal in plants after Fe (Broadley et al. 2007). It is important for the synthesis of proteins, membrane integrity and detoxification, a cofactor for more than 300 proteins, and is found in all six classes of enzymes (Kaur and Garg 2021).

Weathering of parental rock is the main source of Zn in soil, with availability largely determined by the pH value, being higher in acid soils, and leading to Zn deficiency in calcareous soils (Marschner 2012). Zinc deficiency is acerbated in soils with low organic matter content (Broadley et al. 2007), limiting plant growth and crop yield, up to 30% (Alloway 2009). The average concentrations of Zn in most 'normal' soils range between $10-300 \mu g g^{-1}$ (Alloway 2008), but can be in excess of 100,000 µg g⁻¹ in rare calamine soils (metalliferous soils highly enriched in Zn, Pb and Cd) (Cappuyns et al. 2006), where most Znhyperaccumulator plants occur. However, in a number of species, including Arabidopsis halleri (L.) O'Kane & Al-Shehbaz and Noccaea caerulescens (J.Presl & C.Presl) F.K.Mey., can attain hyperaccumulationlevel of Zn while growing in soils with background concentrations of Zn. In A. halleri, concentrations of up to 53,900 μ g g⁻¹, the highest Zn foliar concentration recorded to date, was found while it grew in normal soils with only 342 µg g⁻¹ Zn (Stein et al. 2017). Similarly, Zn concentrations in the leaves of N. caerulescens growing on a soil with only 139 µg g⁻¹ Zn reached up to $\sim 9000 \,\mu g \, g^{-1}$ (Reeves et al. 2001). Similar in C. waldsteinii foliar Zn concentration of>2000 µg g⁻¹ were reported in a plant growing on a soil with 66.1 μg g⁻¹ Zn (Jakovljević et al. 2023). Apart from Zn hyperaccumulation identified in herbarium specimens of *C. waldsteinii*, trace element hyperaccumulation is rare in other *Cardamine* species, found only in *C. hupingshanensis* K.M.Liu, L.B.Chen, H.F.Bai & L.H.Liu, a hyperaccumulator of selenium (Se) from China (Zhou et al. 2018).

In the current study, we aim to determine the ability of Zn hyperaccumulation in wild populations of C. waldsteinii in the Western Balkans. Furthermore, we aim to elucidate the internal distribution of Zn in plant organs of C. waldsteinii using synchrotron micro-X-ray fluorescence elemental imaging (μ XRF). In particular, we are interested to learn whether the patterns of Zn localisation are different compared to other well-studied Zn hyperaccumulators, such as *Noccaea* spp. and *Sedum plumbizincicola*.

Materials and methods

Collection of samples in the field and processing for elemental analysis

The samples of *C. waldsteinii* (Fig. 1) and the associated rhizospheric soil (the soil around the roots of



Fig. 1 Flowering plant of *Cardamine waldsteinii* growing in its natural habitat on limestone near Mt. Medvednica, Croatia



each collected plants at a depth of $\sim 5-10$ cm) (n=3 in SP1-SP7; n=5 in SP8-SP12) were collected from localities in Croatia and Bosnia and Herzegovina, representing the core of the species distribution area (Sabovljević et al. 2025). The additional sample, cultivated at the Loki Schmidt Botanical Garden in Hamburg, Germany, was collected for the synchrotron μXRF analysis. The details on the collection localities are provided in Fig. 2. After initial air-drying in the field, the plant samples were oven-dried at 60 °C for 5 days and subjected to a thorough cleaning to remove the superficial dust with hexane washing according to the protocols of Reeves and Kruckeberg (2018) and Paul et al. (2019). In short, the plant material samples (~1 g) was immersed in 20 mL of anhydrous hexane (HPLC-grade, ≥95%, Sigma-Aldrich) in 50 mL polypropylene tubes, subjected to sonication, extracted from the hexane and dried prior powdering. The plant material was ground to a fine powder (<200 µm) in an impact mill (IKA TubeMill 100 Control). The soil samples were air-dried for 4 days until constant weight and sieved to < 500 µm using a stainless mesh screen (Royal Eijkelkamp Sieve Set Ø 200 mm).

Elemental analysis of plant and soil material samples

For the bulk monochromatic X-ray fluorescence (MXRF) analysis, powdered plant material (0.3 g subsamples) was placed into custom MXRF sample holders and covered with 6.0 µm thin polypropylene film (Chemplex Industries Inc.), while sieved 0.2 g subsamples of the soil were placed in custom XRF sample holders and covered with an 6.0 µm thin polypropylene film (Chemplex Industries Inc.). The MXRF analysis of the plant and soil powdered material were performed using a Z-Spec JP500 instrument (Z-Spec Inc.) in 'Plant' and 'Soil' mode, respectively (Kahlon et al. 2024; Zhang et al. 2025). These modes

SP13	Sampling point	Country	Locality	Altitude (m a.s.l.)	Latitude (°)	Longitude (°)
Legion Germany	SP1	Bosnia and Herzegovina	Prosara, Medjedja	127	45.1957	16.9584
Servembourg Property	SP2	Bosnia and Herzegovina	Banovići, Željova River	447	44.3654	18.4488
	SP3	Bosnia and Herzegovina	Teslić, Vrućica Spa	326	44.5894	17.8862
Switzerlands Final Company	SP4	Bosnia and Herzegovina	Klekovača, Oštrelj	1083	44.4798	16.4092
Stovena	SP5	Bosnia and Herzegovina	Vlasenica, Cvijetanj	511	44.1988	18.9095
Conn.	SP6	Bosnia and Herzegovina	Motajica, Osovica	208	45.0472	17.7066
Nonbeo Para III	SP7	Bosnia and Herzegovina	Kozara, Moštanica	373	45.0632	16.8827
	SP8	Croatia	Velika Kapela, Klek	661	45.2447	15.1489
SP11 SP10	SP9	Croatia	Plitvice, Prijeboj-Ličko Petrovo Selo	643	44.8567	15.6926
SP12 SP8 SP1	SP10	Croatia	Medvednica Nature Park	852	45.8868	15.9282
SP9 SP7 SP6	SP11	Croatia	Mt Ivanšćica	815	46.1942	16.1047
SP4 SP3 SP2 SP5	SP12	Croatia	Žumberak-Samoborsko Gorje Nature Park	980	45.7503	15.3115
CO. ST. DOS AND ADDRESS.	SP13	Germany	Loki Schmidt Botanical Garden, Hamburg	48	53.5660	9.8606

Fig. 2 Distribution and characterisation of sample points (SP) of Cardamine waldsteinii

utilize different Fundemental Parameters in the equation used to convert raw fluorescence counts to concentration values expressed in μg g⁻¹. This equation takes into account bulk composition, density and thickness of the sample. This instrumentation uses monochromatic X-ray fluorescence excitation at 17.48 keV to analyse elements Z=13 (Al) to Z=40 (Zr) on the K-lines and up to Z=92 (U) on the L-lines with optimum sensitivity for elements Cu–Se and Hg-Tl-Pb with LODs ranging from 0.009–0.025 μg g⁻¹. Quality controls included NIST SRM 1570a Trace elements in spinach leaves and NIST SRM 1573a Tomato leaves.

Synchrotron µXRF elemental imaging

Cardamine waldsteinii only flowers and bares leaves for a short time in spring and the large distance travelling between wild localities where it occurs in Bosnia and Herzegovina and Croatia, and the synchrotron facility in Hamburg, made it impossible to get live samples from a natural population. However, C. waldsteinii is cultivated on normal (i.e., not Zn-enriched soil) soil at the Loki Schmidt Botanical Garden in Hamburg. Therefore, a live plant specimen was collected from this locality and used for the synchrotron µXRF elemental imaging described below. The synchrotron micro-X-ray fluorescence (µXRF) experiments were performed at PETRA III (Deutsches Elektronen-Synchrotron DESY), a 6 GeV synchrotron radiation source, specifically at the hard X-ray microprobe undulator beamline P06 (Boesenberg et al. 2016). This beamline is equipped with a cryogenically cooled double-crystal monochromator with Si(111) crystals and using different focusing optics, the X-ray beam can be focused down to sub-micron level. An ion chamber upstream of the sample is used to monitor the incoming flux, while a 500 µm thick Si PIPS diode with an active area of 19 mm diameter (PD300-500CB, Mirion Technologies (Canberra) GmbH, Germany) located downstream of the sample can be used to record the transmitted X-ray intensity to obtain absorption data. Multiple XRF detectors enable the measurement of X-ray fluorescence data. The incident X-ray energy was 15 keV for the entire experiment and focussed with K-B mirrors to 2.1×1.0 um (h×v) with prefocusing, resulting in a flux of ~1.0¹¹ ph/s in the focus. For XRF detection, both a Vortex ME4 (4 elements) in 45° geometry and Vortex ME (1 element, 2 mm thick) in 315° geometry with Xspress3 pulse processors were used. The live plant specimen from the Loki Schmidt Botanical Garden was used to elemental maps of whole plant organs. These were excised and directly mounted between two sheets of thin film (4.0 µm thickness) stretched over a 3D printed plastic frame holder to prevent dehydration during the measurement. Thin sections of the root, stem, and petiole were made by hand cutting with a new stainless steel razor blade for each specimen. This 'dry knife' method allow to obtain 0.2-0.5 mm thick sections without any chemical fixing, embedding or water immersion; thereby avoiding elemental deportment. The sections were immediately lifted from the razorblade with a fine-tip brush and deposited onto thin film (Ultralene® Window Film) of 4.0 µm thickness (Cole-Parmer SamplePrep 3525) stretched over the sample holder and covered directly afterwards with another layer of thin film using sticky tape around the samples to make a tight 'sandwhich'. The synchrotron µXRF elemental imaging then took place within 15 min.

Data processing and statistical analyses

The data acquisition was handled by a custom workflow (Garrevoet 2025) and the XRF data were processed using non-linear least squares fitting as implemented in PyMCA (Solé et al. 2007). This produced 32-bit.tiff images with pixel values corresponding to µg cm⁻² areal density of the element of interest. The figures were prepared in ImageJ (Schneider et al. 2012) by changing the lookup table (LUT) to 'Fire' and adjusting the pixel intensity value range with the levels slider such that background is scaled black and highest concentration values are scaled in the highest range of the LUT (nearly white). Finally, concentration scale bars using the 'calibration' tool and length scales were added.

Results

Zinc accumulation in field specimens

The roots and leaves of *C. waldsteinii* and associated rhizospheric soils were analysed and the mean and ranges of key elements are shown in Tables 1 and S1. The elemental concentrations in the soil samples



Table 1 Zinc concentrations in soil and plant samples of *Cardamine waldsteinii*. Data are expressed in μg g⁻¹ as range and mean values. See Fig. 2 for the sampling point locations

Sample	Soil		Roots		Leaves	
	ranges	means	ranges	means	ranges	means
SP1	n.a	74.8	618–1310	860	1860-2560	2110
SP2	n.a	77.2	2080-4210	2870	3300-5650	4160
SP3	n.a	93.3	521-2450	955	721-3450	1430
SP4	n.a	108	562-1250	842	1390-4440	2990
SP5	n.a	99.9	697-1940	1160	2540-3640	2930
SP6	n.a	112	3250-6210	5170	1920-9260	7190
SP7	n.a	84.8	646-3080	2060	1140-5970	3490
SP8	165-240	184	1200-5810	3410	2320-9610	5530
SP9	117-165	146	1200-2210	1780	3240-5890	4980
SP10	78.9-137	110	n.a	n.a	1440-4370	2510
SP11	98.1-197	158	n.a	n.a	3120-7000	4580
SP12	27.4-89.9	73.5	n.a	n.a	1210-3260	2220
SP13	n.a	n.a	n.a	6090	1870-5220	3820

n.a.: data not available

varied in a similar range for all of the elements analysed, including Zn which ranged from 74 to 184 μg g⁻¹. The same applies to the plant samples, in which the trace elemental concentrations (with the exception of Zn) proved to be unremarkable (Table S1). Foliar Zn concentrations in *C. waldsteinii* individuals were up to>9000 μg g⁻¹ Zn and exceeded the hyperaccumulation threshold in almost all populations (except for SP1; Table 1) in at least one individual. Foliar Zn concentrations also exceeded those in the roots in all naturally grown populations (TF>1), indicating a strong affinity for Zn translocation. This potential was confirmed by high values of the BCF, ranging from 15.3 (SP3) to 64.5 (SP6) (Table S2).

Elemental distribution in plant organs and tissues

The synchrotron µXRF elemental Zn maps of *C. waldsteinii* roots revealed predominant localisation in the main root, and a lower prevailing concentrations in the secondary roots. There was a non-distinct distribution of Zn in the root cortex, with a slightly higher Zn enrichment in the nodes of the lateral branches (Fig. 3). The epidermis was also an important localisation sites for Zn, but with a discontinuous distribution and higher concentrations in the proximal parts of the roots. Zinc accumulation in the epidermis was also observed in the root cross-section, but with significantly higher concentrations in the vascular bundles and endodermis, and some enrichment in the pericycle (Fig. 4A). In

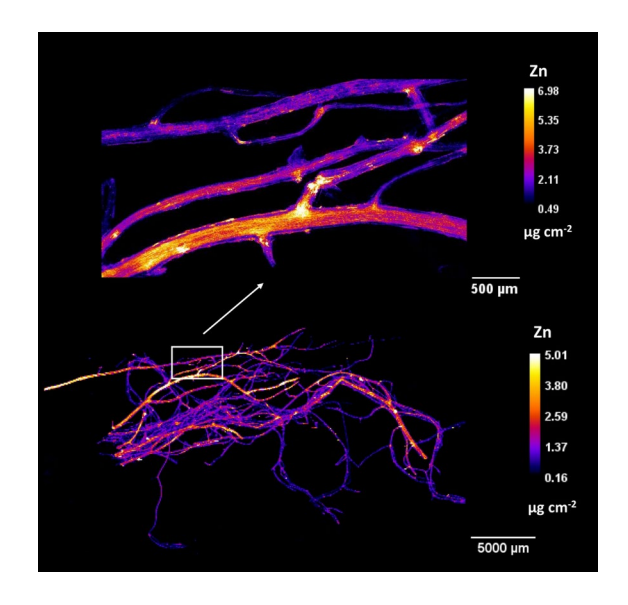


Fig. 3 Synchrotron μ XRF elemental maps showing the distribution of Zn in intact roots of *Cardamine waldsteinii*. The elemental map was acquired at 5 μ m (upper part) and 80 μ m (lower part) step sizes with 5 ms (upper part) and 8 ms (lower part) dwell time per pixel. Scale and concentration bars are included.

the stem and petiole of *C. waldsteinii*, the epidermis had lower Zn concentrations (Fig. 4B and C). The pattern of Zn accumulation was the similar in the young and in the mature leaves of *C. waldsteinii*, with higher Zn concentrations in the old ones, and a clear Zn enrichment in the leaf margins, especially at the tip and around the distal veins (Fig. 5). In



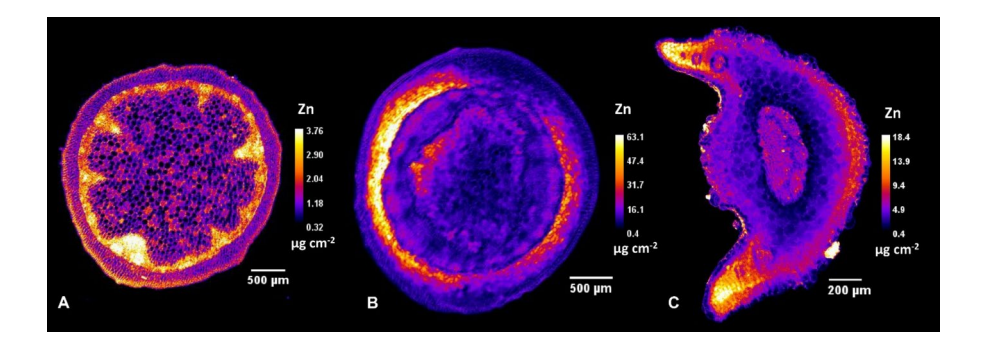


Fig. 4 Synchrotron μ XRF elemental maps showing the distribution of Zn in root A, stem B and petiole C cross-sections of *Cardamine waldsteinii*. The elemental map was acquired

at 10 μ m **A**, 8 μ m **B** and 2.5 μ m **C** step sizes with 8 ms **A** and 5 ms **B**, **C** dwell time per pixel. Scale and concentration bars are included for each specimen.

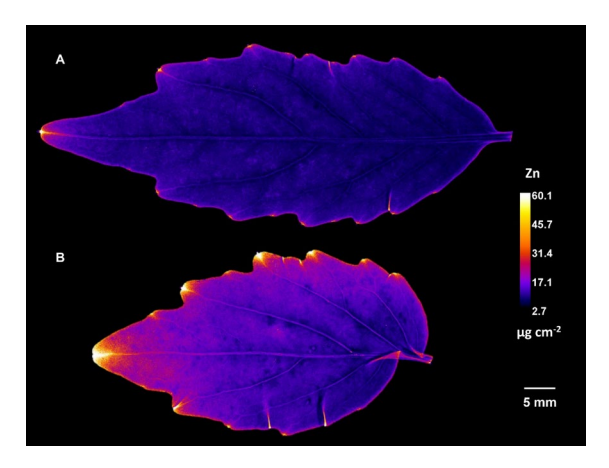


Fig. 5 Synchrotron μ XRF elemental map showing the distribution of Zn in intact young **A** and mature **B** leaves of *Cardamine waldsteinii*. The elemental map was acquired at 33 μ m step size with 7 ms dwell time per pixel. Scale and concentration bars are included.

mature leaves, Zn accumulation was also observed in the peripheral areas of the lamina, with higher prevailing concentrations in the distal parts.

Discussion

The elemental analysis of field collected samples of *C. waldsteinii* confirmed earlier herbarium findings about the potential for Zn hyperaccumulation in this species (Jakovljević et al. 2023). As *C. waldsteinii* can attain in excess of 9000 µg g⁻¹ in its leaves, it clearly is a genuine Zn hyperaccumulator. Soil Zn concentrations were relatively low with

subtle differences between the sampling sites due to the limestone-derived substrate. Consistently high foliar Zn concentrations when C. waldsteinii occurred on soils with $< 240 \mu g g^{-1}$ Zn showed that hyperaccumulation is a constitutive trait in C. waldsteinii. This is akin the well-studied Zn hyperaccumulators A. halleri and N. caerulescens (Bert et al. 2000; Richau and Schat 2009).

The results of this study suggest preferential accumulation of Zn in the vascular bundles of the roots and stems of C. waldsteinii. Preferential accumulation of the hyperaccumulated element in the phloem is a feature in many different hyperaccumulator plant species (Lu et al. 2013; van der Ent et al. 2020). For essential elements such as Zn, this remobilisation is particularly important during plant growth, both for the supply of nutrients to young organs and for the removal of accumulated elements from the old leaves (Marschner 2012). Accumulation of Zn in the vascular bundles of the stem was also observed in Sedum alfredii, another hyperaccumulator of Zn, but only in the hyperaccumulating ecotype, whereas in non-hyperaccumulating ones the epidermis is the main site of accumulation (Tian et al. 2009). In the roots of the hyperaccumulating S. alfredii ecotype, the epidermis and cortex showed to be the main area of Zn accumulation (Gao et al. 2025). The localisation of Zn in the root and stem of C. waldsteinii is similar to the localisation of Zn and Ni in the Ni-hyperaccumulator Noccaea tymphaea (Hausskn.) F.K.Mey. (van der Ent et al. 2019). However, in contrast to the predominant accumulation around the secondary veins of N. tymphaea, Zn in the leaves of C. waldsteinii was mainly



localised in the marginal areas of the leaves. The accumulation of Zn in the marginal areas of the leaf with the highest concentrations in the leaf tips was also observed in *Sedum plumbizincicola* X.H.Guo & S.B.Zhou ex L.H.Wu (Jacquet et al. 2025), another hyperaccumulator of this element. Age-dependent differences in localisation and higher Zn concentrations were observed in the midrib and marginal areas of old leaves of *S. plumbizincicola* (Lu et al. 2014). This contrasts with *C. waldsteinii* where the accumulation of Zn occurs in the same foliar regions, only at different concentrations.

High values of bioaccumulation factors, indicative of a highly efficient Zn uptake even on soils with background concentrations of Zn, and a high leaf-to-root Zn ratio, suggest potential for in Zn biofortification, similar to how *C. hupingshanensis*, the Se hyperaccumulator, has already been extensively used for Se biofortification in China (Wang et al. 2024). Finally, this study highlights the need for a comprehensive study of the ionome of the species of the genus *Cardamine* (with over 200 species known worldwide) with the aim of discovering new metal/metalloid hyperaccumulator species.

Acknowledgements We acknowledge DESY (Hamburg, Germany), a member of the Helmholtz Association HGF, for the provision of experimental facilities. Parts of this research were carried out at PETRA III. Data was collected using beamline P06 operated/provided by DESY Photon Science. This research was supported in part through the Maxwell computational resources operated at Deutsches Elektronen-Synchrotron DESY, Hamburg, Germany. We would like to thank Dennis Brueckner for assistance in using beamline P06 and for performing the XRF data processing. We thank the Loki Schmidt Botanical Garden for donation of the *C. waldsteinii* specimen used in this study.

Author contributions SB and SŠ collected the samples in the field. MS prepared the samples and conducted the analysis. AvdE, KJ, MS and TM conducted the synchrotron μ XRF experiment. KJ and AvdE wrote the first draft of the manuscript. All authors reviewed and approved the final draft of the manuscript.

Funding This work was supported by Ministry of Science Technological Development and Innovation of the Republic of Serbia (Grant Numbers 451–03-136/2025–03/200007 and 451–03-65/2024–03/200178) and by the Faculty of Agriculture, University of Zagreb.

Data availability The data that support this study will be shared upon reasonable request to the corresponding author.

Declarations

Conflicts of interest The authors declare no conflicts of interest relevant to the content of this manuscript.

Open Access This article is licensed under a Creative Commons Attribution 4.0 International License, which permits use, sharing, adaptation, distribution and reproduction in any medium or format, as long as you give appropriate credit to the original author(s) and the source, provide a link to the Creative Commons licence, and indicate if changes were made. The images or other third party material in this article are included in the article's Creative Commons licence, unless indicated otherwise in a credit line to the material. If material is not included in the article's Creative Commons licence and your intended use is not permitted by statutory regulation or exceeds the permitted use, you will need to obtain permission directly from the copyright holder. To view a copy of this licence, visit https://creativecommons.org/licenses/by/4.0/.

References

- Alloway BJ (2008) Zinc in Soils and Crop Nutrition, 2nd edn. International Zinc Association and International Fertilizer Industry Association, Brussels
- Alloway BJ (2009) Soil factors associated with zinc deficiency in crops and humans. Environ Geochem Health 31(5):537–548. https://doi.org/10.1007/s10653-009-9255-4
- Bert V, Macnair MR, De Laguerie P, Saumitou-Laprade P, Petit D (2000) Zinc tolerance and accumulation in metallicolous and nonmetallicolous populations of *Arabidopsis halleri* (Brassicaceae). New Phytol 146(2):225–233. https://doi.org/10.1046/j.1469-8137.2000.00634.x
- Boesenberg U, Ryan CG, Kirkham R, Siddons DP, Alfeld M, Garrevoet J, Núñez T, Claussen T, Kracht T, Falkenberg G (2016) Fast X-ray microfluorescence imaging with submicrometer-resolution integrating a Maia detector at beamline P06 at PETRA III. J Synchrotron Rad 23:1550–1560. https://doi.org/10.1107/S1600577516015289
- Broadley MR, White PJ, Hammond JP, Zelko I, Lux A (2007) Zinc in plants. New Phytol 173(4):677–702. https://doi. org/10.1111/j.1469-8137.2007.01996.x
- Cappuyns V, Swennen R, Vandamme A, Niclaes M (2006) Environmental impact of the former Pb–Zn mining and smelting in East Belgium. J Geochem Explor 88(1–3):6– 9. https://doi.org/10.1016/j.gexplo.2005.08.005
- Gao Y, Yu H, Liu X, Lin H, Lu L (2025) Mechanisms involved in the positive effects of high zinc exposure on growth of *Sedum alfredii*. Plant Soil 507(1):823–843. https://doi.org/ 10.1007/s11104-024-06773-w
- Garrevoet J (2025) A framework for data processing used at the hard X-ray micro/nano probe at PETRA III based on micro-services. J Phys Conf Ser 3010:012136. https://doi.org/10.1088/1742-6596/3010/1/012136
- Jacquet J, Jakovljević K, Brueckner D, Sirguey C, van der Ent A (2025) Synchrotron elemental imaging reveals zinc distribution in the hyperaccumulator Sedum plumbizincicola (Crassulaceae). Ecol Res. In Press. https://doi.org/10. 1111/1440-1703.70019



- Jakovljević K, Mišljenović T, van der Ent A, Baker AJM, Andrejić G, Tomović G, Echevarria G (2023) Zinc (hyper) accumulation in *Cardamine waldsteinii*: from discovery in the herbarium to validation in the field. Plant Biosyst 157(4):851–857. https://doi.org/10.1080/11263504.2023. 2204318
- Kahlon PS, Kokkinopoulou P, Alfageme SB, Leong CK, Chen Z, Testerink C, van der Ent A (2024) Quantitative light element (sodium–calcium) profiling in plant tissues using monochromatic X-ray fluorescence analysis. bioRxiv 2024–10. https://doi.org/10.1101/2024.10.22.619597
- Kaur H, Garg N (2021) Zinc toxicity in plants: a review. Planta 253(6):129. https://doi.org/10.1007/s00425-021-03642-z
- Lu L, Tian S, Zhang J, Yang X, Labavitch JM, Webb SM, Latimer M, Brown PH (2013) Efficient xylem transport and phloem remobilization of Zn in the hyperaccumulator plant species *Sedum alfredii*. New Phytol 198(3):721–731. https://doi.org/10.1111/nph.12168
- Lu L, Liao X, Labavitch J, Yang X, Nelson E, Du Y, Brown PH, Tian S (2014) Speciation and localization of Zn in the hyperaccumulator *Sedum alfredii* by extended X-ray absorption fine structure and micro-X-ray fluorescence. Plant Physiol Biochem 84:224–232. https://doi.org/10.1016/j.plaphy.2014.10.004
- Marschner H (2012) Marschner's mineral nutrition of higher plants. Academic press, Elsevier
- Paul AL, van der Ent A, Erskine PD (2019) Scandium biogeochemistry at the ultramafic Lucknow deposit, Queensland, Australia. J Geochem Explor 204:74–82. https://doi.org/ 10.1016/j.gexplo.2019.05.005
- Reeves RD, Kruckeberg AR (2018) Re-examination of the elemental composition of some Caryophyllaceae on North American ultramafic soils. Ecol Res 33:715–722. https:// doi.org/10.1007/s11284-017-1556-y
- Reeves RD, Schwartz C, Morel JL, Edmondson J (2001) Distribution and metal-accumulating behavior of *Thlaspi caerulescens* and associated metallophytes in France. Int J Phytoremediation 3(2):145–172. https://doi.org/10.1080/15226510108500054
- Reeves RD, Baker AJM, Jaffré T, Erskine PD, Echevarria G, van der Ent A (2018) A global database for hyperaccumulator plants of metal and metalloid trace elements. New Phytol 218:407–411. https://www.jstor.org/stable/90019919
- Richau KH, Schat H (2009) Intraspecific variation of nickel and zinc accumulation and tolerance in the hyperaccumulator *Thlaspi caerulescens*. Plant Soil 314:253–262. https://doi.org/10.1007/s11104-008-9724-z
- Sabovljević M, Tomović G, Djordjević V, Stanković S, Sabovljević A et al (2025) New records and noteworthy data of plants, algae and fungi in SE Europe and adjacent regions, 23. Compr Plant Biol 49(2):309–327. https://doi. org/10.2298/CPB2502309S
- Schneider CA, Rasband WS, Eliceiri KW (2012) NIH image to ImageJ: 25 years of image analysis. Nat Methods 9(7):671–675. https://doi.org/10.1038/nmeth.2089

- Solé VA, Papillon E, Cotte M, Walter Ph, Susini J (2007) A multiplatform code for the analysis of energy-dispersive X-ray fluorescence spectra. Spectrochim Acta B 62:63– 68. https://doi.org/10.1016/j.sab.2006.12.002
- Stein RJ, Höreth S, de Melo JRF, Syllwasschy L, Lee G, Garbin ML, Clemens S, Krämer U (2017) Relationships between soil and leaf mineral composition are element-specific, environment-dependent and geographically structured in the emerging model *Arabidopsis halleri*. New Phytol 213(3):1274–1286. https://doi.org/10.1111/nph.14219
- Tian SK, Lu LL, Yang XE, Labavitch JM, Huang YY, Brown P (2009) Stem and leaf sequestration of zinc at the cellular level in the hyperaccumulator *Sedum alfredii*. New Phytol 182(1):116–126. https://doi.org/10.1111/j.1469-8137. 2008.02740.x
- van der Ent A, Baker AJM, Reeves RD, Pollard AJ, Schat H (2013) Hyperaccumulators of metal and metalloid trace elements: facts and fiction. Plant Soil 362(1–2):319–334. https://doi.org/10.1007/s11104-012-1287-3
- van der Ent A, Spiers KM, Brueckner D, Echevarria G, Aarts MG, Montargès-Pelletier E (2019) Spatially-resolved localization and chemical speciation of nickel and zinc in *Noccaea tymphaea* and *Bornmuellera emarginata*. Metallomics 11(12):2052–2065. https://doi.org/10.1039/c9mt00106a
- van der Ent A, de Jonge MD, Mak R, Mesjasz-Przybyłowicz J, Przybyłowicz WJ, Barnabas AD, Harris HH (2020) X-ray fluorescence elemental mapping of roots, stems and leaves of the nickel hyperaccumulators *Rinorea* cf. *bengalensis* and *Rinorea* cf. *javanica* (Violaceae) from Sabah (Malaysia), Borneo. Plant Soil 448:15–36. https://doi.org/10.1007/s11104-019-04386-2
- Wang L, Li S, Wang F, Zhang N, Chen X, Wang X, He J, Cheng C, Zhu Z (2024) A se-hyperaccumulating plant Cardamine violifolia: from its nutritional value to potential applications in foods. Trends Food Sci Technol 154:104781. https://doi.org/10.1016/j.tifs.2024.104781
- Zhang C, Charrois L, Jacquet J, Sirguey C, Chen Z, van der Ent A (2025) Monochromatic X-ray fluorescence spectroscopy for major and trace element analysis in plant science applications. Plant Soil. In Press. https://doi.org/10.1007/ s11104-025-07984-5
- Zhou Y, Tang Q, Wu M, Mou D, Liu H, Wang S, Zhang C, Ding L, Luo J (2018) Comparative transcriptomics provides novel insights into the mechanisms of selenium tolerance in the hyperaccumulator plant *Cardamine hupingshanensis*. Sci Rep 8(1):2789. https://doi.org/10.1038/s41598-018-21268-2

Publisher's Note Springer Nature remains neutral with regard to jurisdictional claims in published maps and institutional affiliations.



Terms and Conditions

Springer Nature journal content, brought to you courtesy of Springer Nature Customer Service Center GmbH ("Springer Nature"). Springer Nature supports a reasonable amount of sharing of research papers by authors, subscribers and authorised users ("Users"), for small-scale personal, non-commercial use provided that all copyright, trade and service marks and other proprietary notices are maintained. By accessing, sharing, receiving or otherwise using the Springer Nature journal content you agree to these terms of use ("Terms"). For these purposes, Springer Nature considers academic use (by researchers and students) to be non-commercial.

These Terms are supplementary and will apply in addition to any applicable website terms and conditions, a relevant site licence or a personal subscription. These Terms will prevail over any conflict or ambiguity with regards to the relevant terms, a site licence or a personal subscription (to the extent of the conflict or ambiguity only). For Creative Commons-licensed articles, the terms of the Creative Commons license used will apply.

We collect and use personal data to provide access to the Springer Nature journal content. We may also use these personal data internally within ResearchGate and Springer Nature and as agreed share it, in an anonymised way, for purposes of tracking, analysis and reporting. We will not otherwise disclose your personal data outside the ResearchGate or the Springer Nature group of companies unless we have your permission as detailed in the Privacy Policy.

While Users may use the Springer Nature journal content for small scale, personal non-commercial use, it is important to note that Users may not:

- 1. use such content for the purpose of providing other users with access on a regular or large scale basis or as a means to circumvent access control;
- 2. use such content where to do so would be considered a criminal or statutory offence in any jurisdiction, or gives rise to civil liability, or is otherwise unlawful;
- 3. falsely or misleadingly imply or suggest endorsement, approval, sponsorship, or association unless explicitly agreed to by Springer Nature in writing;
- 4. use bots or other automated methods to access the content or redirect messages
- 5. override any security feature or exclusionary protocol; or
- 6. share the content in order to create substitute for Springer Nature products or services or a systematic database of Springer Nature journal content.

In line with the restriction against commercial use, Springer Nature does not permit the creation of a product or service that creates revenue, royalties, rent or income from our content or its inclusion as part of a paid for service or for other commercial gain. Springer Nature journal content cannot be used for inter-library loans and librarians may not upload Springer Nature journal content on a large scale into their, or any other, institutional repository.

These terms of use are reviewed regularly and may be amended at any time. Springer Nature is not obligated to publish any information or content on this website and may remove it or features or functionality at our sole discretion, at any time with or without notice. Springer Nature may revoke this licence to you at any time and remove access to any copies of the Springer Nature journal content which have been saved.

To the fullest extent permitted by law, Springer Nature makes no warranties, representations or guarantees to Users, either express or implied with respect to the Springer nature journal content and all parties disclaim and waive any implied warranties or warranties imposed by law, including merchantability or fitness for any particular purpose.

Please note that these rights do not automatically extend to content, data or other material published by Springer Nature that may be licensed from third parties.

If you would like to use or distribute our Springer Nature journal content to a wider audience or on a regular basis or in any other manner not expressly permitted by these Terms, please contact Springer Nature at

onlineservice@springernature.com